Solid-state synthesis of $LnOCl/Ln_2O_3$ (Ln = Eu, Nd) by using Chitosan and PS-*co*-P4VP as polymeric supports.

C. Diaz[1,*], Daniel Carrillo[1], R. de la Campa[2], A. Presa Soto[2] and M. L. Valenzuela[3*]

1. Departamento de Química, Facultad de Química, Universidad de Chile. La Palmeras 3425, Nuñoa, casilla 653, Santiago de Chile, Chile; 2. Departamento de Química Orgánica e Inorgánica (IUQOEM). Facultad de Química. Universidad de Oviedo. Julián Clavería s/n, 33006, Oviedo, Spain; 3.Universidad Autónoma de Chile, Facultad de Ingeniería, Instituto de Ciencias Químicas Aplicadas, Inorganic Chemistry and Molecular Material Center. Av. El Llano Subercaseaux 2801, Santiago de Chile).

Abstract

Series of lanthanide materials of type LnOCl or Ln_2O_3 (Ln = Eu, Nd) are successfully prepared via a convenient and straightforward two-step procedure. Firstly, and by using Chitosan and PS-*co*-P4VP as polymeric supports, macromolecular complexes of type Chitosan●$LnCl_3$ and PS-*co*-P4VP●$LnCl_3$ are prepared. These macromolecular complexes were treated in solid state at 800 °C under air, leading to the corresponding LnOCl or Ln_2O_3 materials (Ln = Eu, Nd) with moderate to good yields. The nature of the as prepared lanthanide materials (LnOCl and/or Ln_2O_3) is strongly influenced by the polymeric template (i.e., Chitosan or PS-*co*-P4VP), the lanthanide salt precursor, and the polymer/lanthanide molar ratio. Thus, when Chitosan●$EuCl_3$ and PS-*co*-P4VP●$EuCl_3$ are used as macromolecular precursors, a mixture of crystalline phases of both EuOCl and Eu_2O_3 are obtained. However, when Chitosan●$NdCl_3$ and PS-*co*-P4VP●$NdCl_3$ are used, a sole pure crystalline phase of NdOCl is obtained. The nanostructured lanthanide materials have been characterized by means of XRD (X-ray diffraction of powder), SEM, EDS, TEM, and HRTEM. The luminescent spectra of the as prepared $EuOCl/Eu_2O_3$ mixture materials show an emission pattern whose intensity is strongly influenced by the nature of the polymeric precursor, as well as on the metal/polymer molar ratios.

Keywords: $EuOCl/Eu_2O_3$; NdOCl; solventless method; luminescence; lanthanides

Nowadays, nanostructured lanthanide oxychlorides, LnOCl, represent a very interesting class of materials[1,2]. Indeed, LnOCl materials exhibit a high chemical stability and, more importantly, the ability to promote energy transfer processes to dopant ions, specially other lanthanide atoms. These properties have been exploited in several applications such as optical stimulated and field-emission driven phosphors, X-ray detectors, up-conversion lasers, and optical telecommunication infrastructures [1,2]. Most of these applications demand efficient solid-state synthetic routes to nanostructured lanthanide oxychlorides. However, most common synthetic routes to LnOCl materials are based on

solution methodologies[7-13], which usually need of evaporation steps in order to incorporate the lanthanide material into a practical device. However, solvent evaporation steps are frequently accompanied by not desired nanoparticles agglomeration [4-6]. Thus, to date the development of a general solid-state route to LnOX (X = halide) remains challenged [13] (to best of our knowledge, literature only reported one example of solid state synthesis of LnOCl from mixtures of Ln_2O_3 and $LnCl_3$[14]).

Most of research on the synthesis of LnOCl materials have been performed with Ln = La[7], Gd[7,8], Ce[8], and Dy[8]. For instance, nanostructured GdOCl materials were synthesized by both solvothermal and surfactant-assisted methods[7]. Additionally, GdOCl has been recently prepared by heating mixtures of $GdCl_3$, $Gd(O´Pr)_3$, and TOPO, using oleyamine as solvent[8]. However, the synthesis of LnOCl with Ln = Eu[9] and Nd,[10-12] have received significantly less attention. Thus, in the literature there is a sole example of the synthesis of EuOCl microparticles by thermal decomposition of $Eu(OH)_2Cl$[9]. On the other hand, pure NdOCl materials, including nanocubes, were synthesized by Li and co-workers by heating solutions of $NdCl_3{\bullet}6H_2O$ in oleyamine[10]. Furthermore, $NdOCl/SiO_2$ composites have been created by Yue et al. by treating $NdOCl\text{-}SiO_2$ mixtures with NaOH[11]. On the other hand, lanthanide oxides (Ln_2O_3) are a class of lanthanide materials widely used as phosphor for fluorescent lighting, display monitors, optical telecommunications and catalysis[15-18]. Similarly to LnOCl materials, the synthesis of Ln_2O_3 is usually achieved by using solution methods[17,18], being the solid-state routes limited to a solution–solid state route based on a coordination polymer created by the combination of a lanthanide metal and amino acids[8].

Our group has been recently studying different solid-sate routes to nanostructured metal oxides such as V_2O_5[19], Fe_2O_3[20], ZnO[21], SnO_2[21] as well some metal as Pt[22] and mixtures as Pd/PdO[23]. These solid-state routes are based on heating an appropriate macromolecular complex, which has been previously created by mixing a polymeric support and metallic salt. This two-step simple methodology allows the incorporation of the as-prepared materials directly on devices, i.e. without any solvent evaporation steps, which preclude the particle agglomeration or tedious solvent evaporation procedures[7-18]. Thus, we herein show a solid-state route to pure nanostructured NdOCl and $EuOCl/Eu_2O_3$ mixtures, base on thermal treatment of macromolecular precursors Chitosan$\bullet NdCl_3$, PS-*co*-P4VP$\bullet NdCl_3$, Chitosan$\bullet EuCl_3$ and PS-*co*-P4VP$\bullet EuCl_3$. We studied the influence of the nature of the polymer template (Chitosan or PS-*co*-P4VP) and the polymer/Ln ratio on the properties of the as prepared LnOCl and Ln_2O_3. The luminescent properties of the Eu_2O_3 and $EuOCl/Eu_2O_3$ materials were also studied. Although other lanthanide oxides could be potentially prepared by this methodology, in this work, we present the synthesis of those of Nd and Eu due principally to: (i) the lack of synthetic routes to these oxides, and (ii) the very promising applications of these materials (for instance the outstanding emission features, in the visible region of the spectra, of the Eu oxides, make them potential materials to be used in screens, whereas the emission properties of Nd oxides make them potential materials to solid state lasers applications).

1 Experimental

1.1 Synthesis of macromolecular complexes Polymer●($LnCl_3$) (Polymer = Chitosan or PS-*co*-P4VP; Ln = Eu or Nd).

The macromolecular complexes Chitosan●($LnCl_3$) and PS-*co*-P4VP●($LnCl_3$), Ln = Eu and Nd; PS-*co*-P4VP = poly(4-vinylpyridine)-*co*-polystyrene) were prepared according to a previous synthetic methodology described by us for other macromolecular precursors[19-23]. In a typical synthesis, the lanthanide salts and the polymeric support (i.e. chitosan or PS-*co*-P4VP) are placed into a Schlenk tube with CH_2Cl_2, and the mixture was stirred for several days. Then, the solvent was removed under vacuum, obtaining the corresponding macromolecular complexes in very high yields (*ca.* 90 %). Details of the amounts of metallic salts, polymers, and solvent, as well as reaction time, are given in Table 1. Based on our previous experience on the synthesis of nanostructured metal oxides by heating an appropriate metallic macromolecular precursor, in this work the lanthanide salt/Polymer molar ratios were chosen to be 1/1 and 1/5 (previous work showed that molar ratios lower than 1/1 or higher than 1/5 led to material having the same particle size and morphology than those of 1/1 and 1/5)[19-24]. Similarly (i.e. base on our previous results on the synthesis of other nanostructured oxides), the reaction time was optimized to 21 and 14 days to Eu and Nd material respectively[19-24].

Table 1 Experimental details of the synthesis of LnOCl and Ln_2O_3 materials by heating macromolecular complexes Chitosan●($LnCl_3$) and PS-*co*-P4VP●($LnCl_3$) (Ln = Eu, Nd).

Sample	Macromolecular complex	$LnCl_3$/polymer Ln = Eu, Nd	g. Chitosan	g. PS-*co*-P4VP	g. $LnCl_3$	solvent mL	time (days)
1	Chitosan·($EuCl_3$)	1:1	0.24		0.50[(a)]	20	21
2		1:5	1.17		0.50[(a)]	40	21
3	PS-*co*-P4VP·($EuCl_3$)	1:1		0.29	0.50[(a)]	20	21
4		1:5		1.43	0.50[(a)]	40	21
5	Chitosan·($NdCl_3$)	1:1	0.48		1.00[(b)]	20	14
6		1:5	0.58		1.00[(b)]	40	14
7	PS-*co*-P4VP·($NdCl_3$)	1:1		0.58	1.0[(b)]	20	14
8		1:5		2.92	1.0[(b)]	40	14

(a) $EuCl_3$. (b) $NdCl_3$.

1.2 Pyrolysis of the macromolecular complexes Polymer●($LnCl_3$) (Polymer = Chitosan or PS-*co*-P4VP; Ln = Eu or Nd).

Solid samples of Chitosan●($LnCl_3$) and PS-*co*-P4VP●($LnCl_3$), Ln = Eu or Nd, were pyrolized at 800 °C under air atmosphere by using a controlled temperature program (samples were heated from 25 to 800 ºC at a constant heating rate of 10°C/min. Then, samples were heated at 800ºC during 5 hours. All processes were performed in a furnace WiseTherm FHP-12, Daihan Scientific, Co. Ltd). Temperature of 800ºC was chosen for the pyrolitic studies on the base of our previous experience on the synthesis of other nanostructured oxides[19-24].

1.3. Characterization of as prepared EuOCl/Eu_2O_3 and NdOCl

The pyrolyzed samples were characterized by SEM (JSM-6380LV, Jeol Ltd. Microscope), HR-TEM (JEOL 2011, Ltd. Microscope. XRD using a Siemens D-5000 diffractometer with a Cu-Kα radiation of (40 KV, 30 mA)), and a graphite monochromator (λ = 1.540598 Å). Fluorescence spectroscopy was performed using a Jasco FP-8200 fluorimeter with a solid-state accessory.

2 Results and discussion

2.1 X-ray analysis of the EuOCl/Eu_2O_3 and NdOCl

Crystalline phase of the as prepared materials, both pure NdOCl and mixture EuOCl/Eu_2O_3, was studied by X-ray techniques. Thus, Fig. 1 shows the XRD pattern of lanthanide oxides obtained by the pyrolysis of the polymeric precursors Chitosan●$EuCl_3$ ($EuCl_3$/Chitosan = 1/1 black trace; $EuCl_3$/Chitosan = 1/5 red trace), and PS-*co*-P4VP●$EuCl_3$ ($EuCl_3$/PS-*co*-P4VP = 1/1 green trace; $EuCl_3$/PS-*co*-P4VP = 1/5 blue trace). All XRD shows very similar patters corresponding to the presence of mixtures of EuOCl and Eu_2O_3 phases (see squared and circular dots on fig.1). Importantly, although both phases of EuOCl and Eu_2O_3 are presented in all as-prepared materials, the reaction yields Eu_2O_3 as the major product achieved, being the EuOCl phase only significantly observed when the macromolecular PS-*co*-P4VP●$EuCl_3$ (1/5) was used as macromolecular precursor for the pyrolisys (blue trace in fig.1).

The diffraction pattern of the Eu_2O_3 phases can be indexed as a pure body-centered cubic phase of Eu_2O_3 with a space group Ia-3 (206); which is in accordance with Powder Diffraction File No. 03-065-3182. Moreover, similar XRD pattern has been reported for Eu_2O_3 obtained by using solution synthetic routes[18]. The weak diffraction peaks at 2θ = 12.716° and 2θ = 41.876° corresponding to the EuOCl, can be indexed to a tetragonal phase with a space group P4/nmm (129) according to the Powder Diffraction File No. 01-085-0842. Also very similar XRD spectrum has been reported for EuOCl prepared by using a solution method[9].

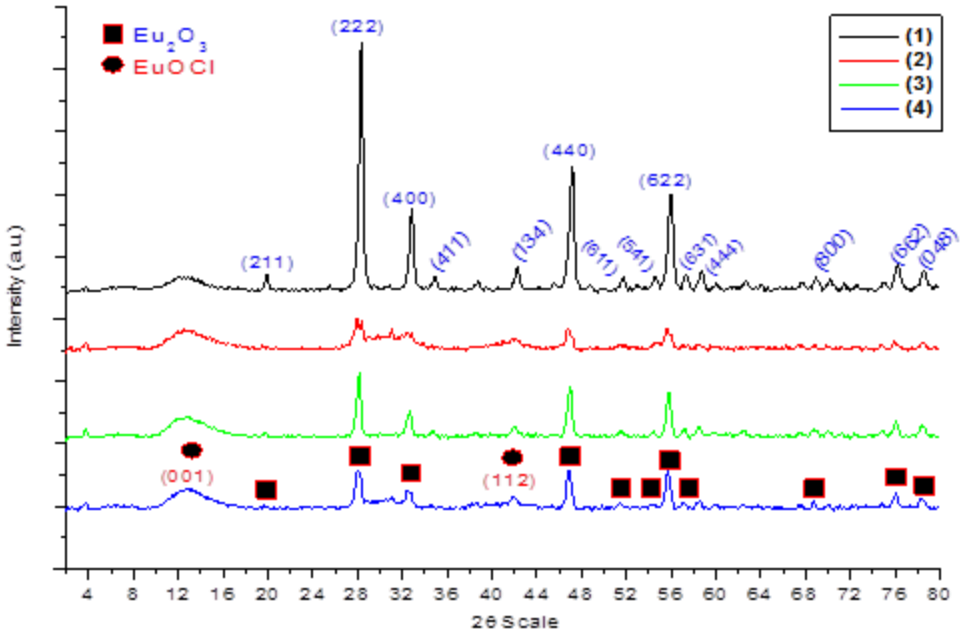

Fig. 1. XRD patterns of the pyrolytic product from Chitosan●$EuCl_3$ and PS-*co*-P4VP●$EuCl_3$ having different polymer/$EuCl_3$ molar ratios: (1) $EuCl_3$/Chitosan = 1/1, black trace. (2) $EuCl_3$/Chitosan = 1/5, red trace. (3) $EuCl_3$/PS-*co*-P4VP = 1/1, green trace. (4) $EuCl_3$/PS-*co*-P4VP = 1/5, blue trace. Eu_2O_3 peaks are indicated with a black square and EuOCl peaks are indicated with a black circle. Non-indexed very small peaks observed at 2θ = 39, 45 and 62º correspond to Eu_2O_3 phases.

The XRD patterns of pyrolytic product obtained from PS-*co*-P4VP●$NdCl_3$ and Chitosan●$NdCl_3$, showed, independently of the polymer/Nd molar ratio, the pure crystalline phase of NdOCl (see fig. 2). The XRD patterns exhibit the main diffraction peaks at 2θ = 13.018°, 26.277°, 31.385°, 34.567°, 41.391°, 45.002°, 51.625°, 52.551°, 54.096°, 57.960θ, 59.123°, 65.821δ, 74.456° and 77.263°, corresponding to the (001), (101), (110), (102), (112), (200), (113), (211), (004), (212), (104), (220), (310) and (214) planes of the NdOCl respectively. A similar XRD pattern was obtained from NdOCl prepared by using synthetic routes in solution [10-12].

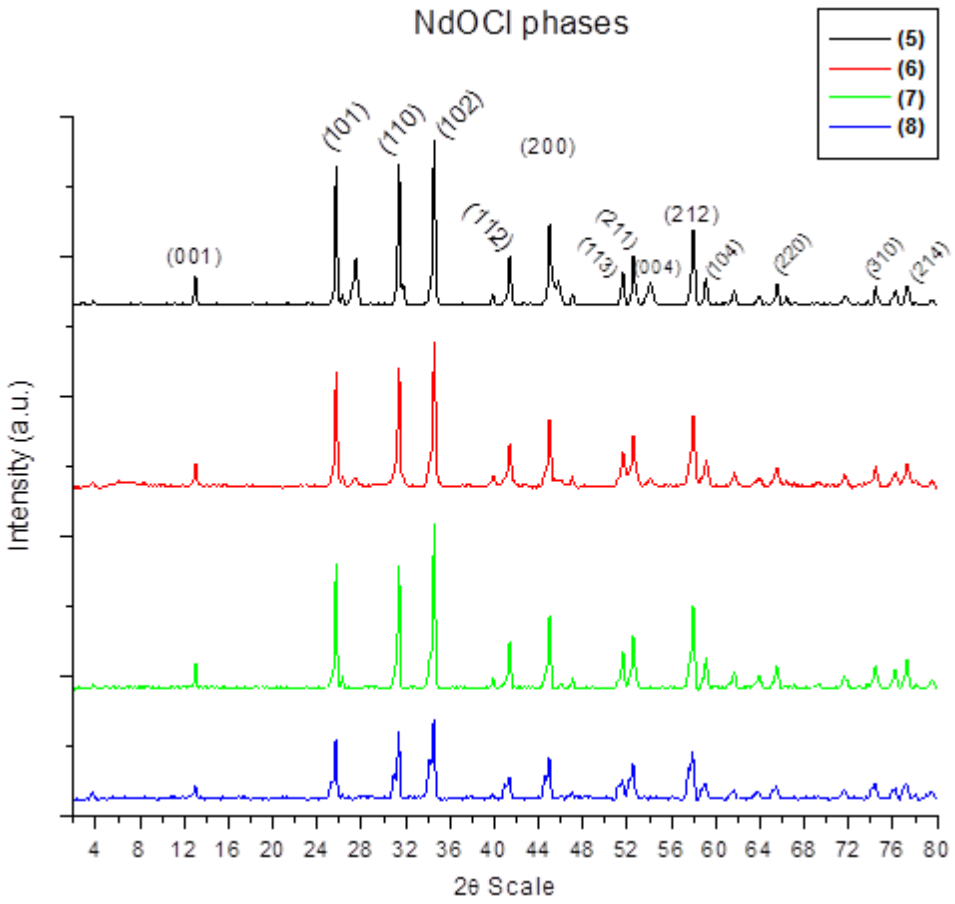

Fig. 2 XRD pattern of the pyrolytic product from Chitosan●$NdCl_3$ and PS-*co*-P4VP●$NdCl_3$ having different polymer/$NdCl_3$ molar ratios: (5) $NdCl_3$/Chitosan = 1/1, black trace. (6) $NdCl_3$/Chitosan = 1/5, red trace. (7) $NdCl_3$/PS-*co*-P4VP = 1/1, green trace. (8) $NdCl_3$/PS-*co*-P4VP = 1/5, blue trace. Non-indexed very small peaks observed at 2θ = 40, 47, 61, 64, and 72º correspond to NdOCl crystallographic phase.

2.2 SEM and TEM analysis of the as-prepared EuOCl/Eu_2O_3 materials.

The morphology and microstructure of the as prepared Eu-containing materials were investigated by SEM and TEM (see fig. 3 and fig. 4). The SEM of the pyrolytic product obtained from the macromolecular precursors Chitosan●$EuCl_3$ (1:1 and 1:5 polymer/Eu molar ratios) and PS-*co*-P4VP●$EuCl_3$ (1:1 polymer/Eu molar ratio) showed very similar porous morphologies (see fig. 3a-c for a representative SEM images of the Eu_2O_3/EuOClmaterials obtained from precursor Chitosan●$EuCl_3$ 1:1). However, the SEM images of the products obtained from the pyrolysis of PS-*co*-P4VP●$EuCl_3$ in 1:5 molar ratio showed a foam-type morphology (see figure 3e-f) corresponding to the mixture of phases of EuOCl/Eu_2O_3. Similar "foam" morphologies has been observed in nanostructured EuOCl/Eu_2O_3 materials synthesized by a solution template methods[18]. EDS analysis (fig. 3d and 3g) of EuOCl/Eu_2O_3 confirmed the presence of Eu and O elements in the structure

of the as prepared materials. Furthermore, the presence of chlorine peak at 2.6 KeV in both EDS spectra confirmed the presence of the EuOCl in the as-prepared materials. However, the low intensity of this peak demonstrated that the major product of these synthetic routes is Eu_2O_3. Furthermore, EDS analysis showed a Eu/O ratio very close to that of 2/3, i.e. that of pure Eu_2O_3 phases, which is also indicative of the small amount of EuOCl presented in as-prepared materials (see Supplementary Material. Note that other small peaks at different values of KeV are also present in DLS spectra corresponding to small impurities. For instance, small peaks at 2.12 and 9.7 keV correspond to Au from the sample holder. See EDS tables in Supplementary Material).

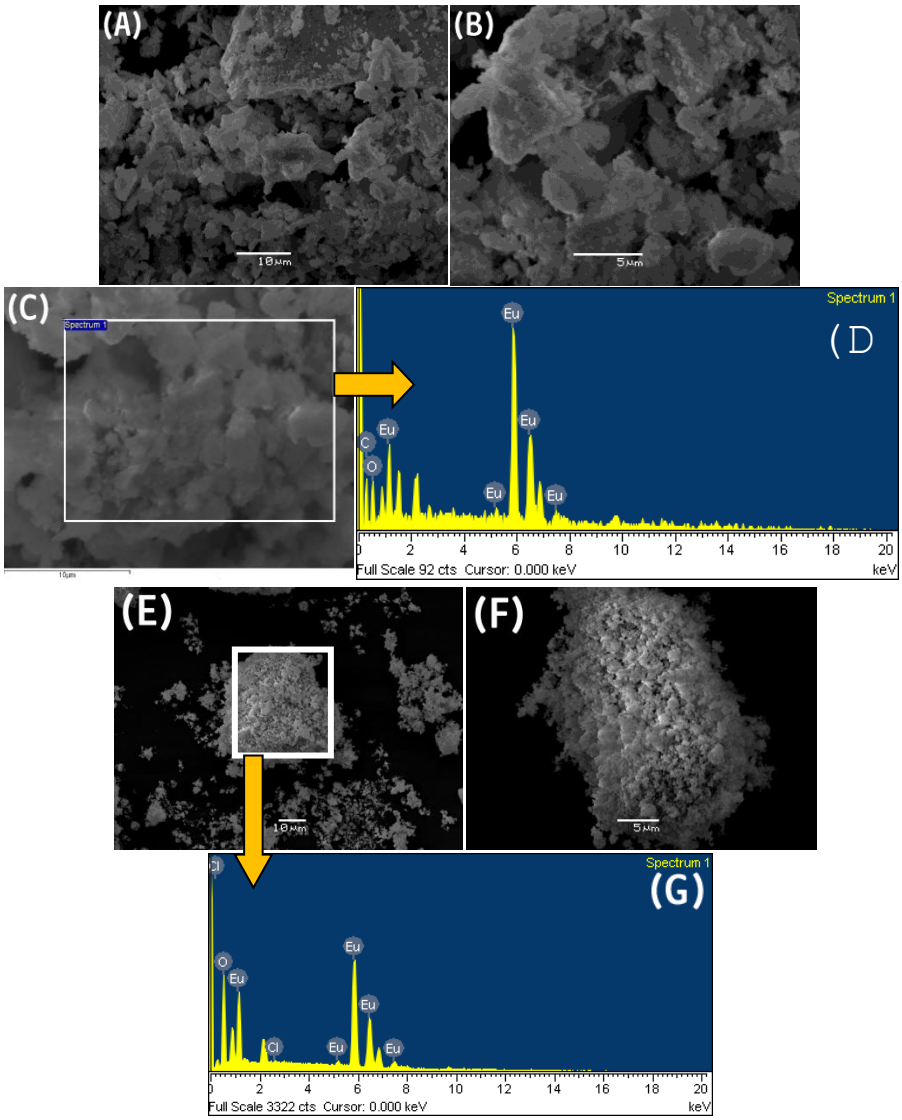

Fig. 3 (a)-(c) SEM images and EDS analysis (d) of the Eu_2O_3 materials prepared from the pyrolysis of the macromolecular precursors Chitosan●$EuCl_3$ 1:1. (e)-(f) SEM images and EDS analysis (g) of the EuOCl/Eu_2O_3 materials prepared by pyrolysis of the macromolecular precursor PS-*co*-P4VP●$EuCl_3$ in molar ratio 1:5.

TEM images of the polymeric precursor Chitosan●$EuCl_3$, in both 1:1 and 1:5 molar ratios, and the PS-*co*-P4VP●$EuCl_3$ in molar ratio 1:1, exhibited the presence of Eu_2O_3 nanoparticles having not well-defined morphologies and sizes (a representative example of the pyrolytic Eu_2O_3/EuOCl materials obtained from the macromolecular precursor Chitosan●$EuCl_3$ in molar ratio 1:1 is shown in fig. 4a-c). However, and in spite of the non well-defined morphologies observed from this synthetic route, the bar-shaped morphology was frequently observed in the TEM images (see red squared regions in fig 4a). The crystalline nature of the as prepared Eu_2O_3/EuOCl materials is clearly demonstrated by the selected area electron diffraction (SAED) pattern (fig. 4d), which showed well-defined crystalline rings.

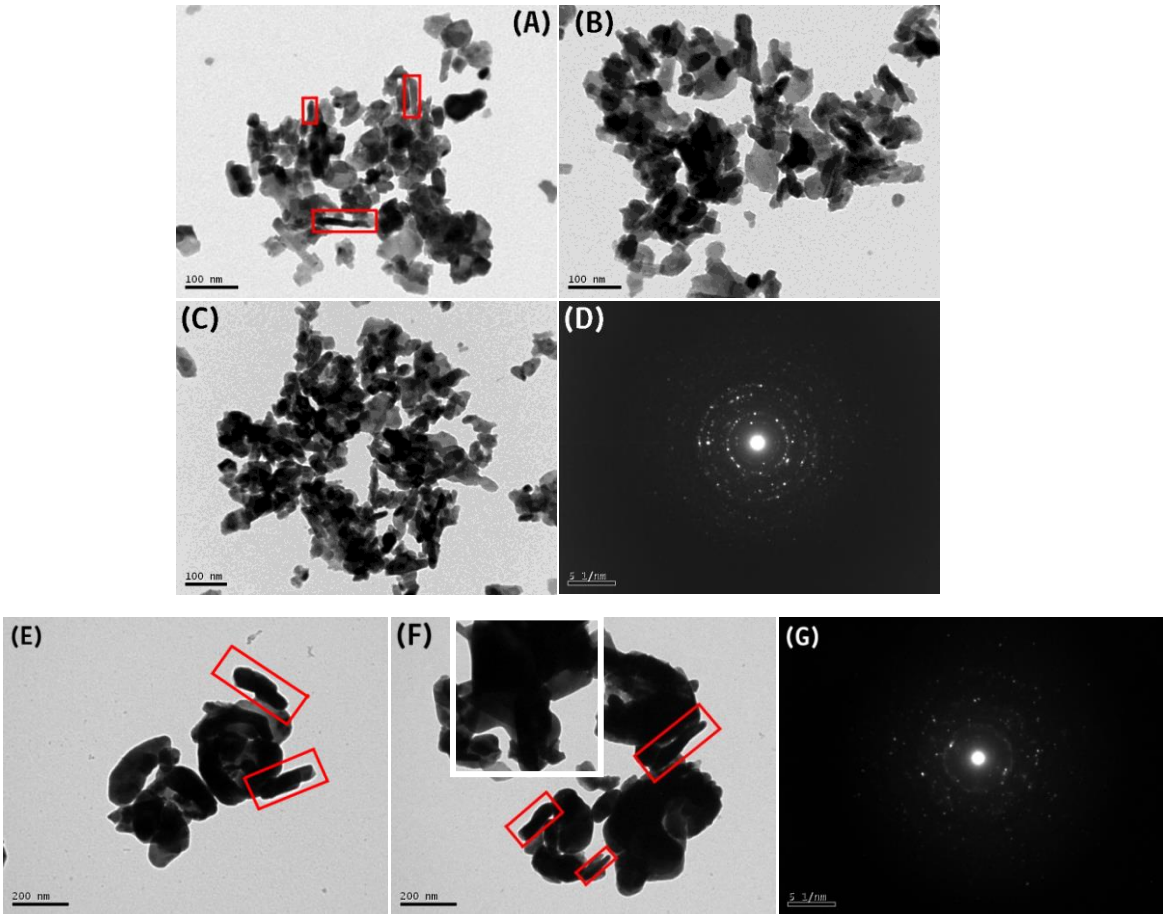

Fig. 4 (a)-(c) TEM images and SAED pattern (d) of the Eu_2O_3 prepared from the macromolecular precursor Chitosan●$EuCl_3$ 1:1. (e), (f) TEM images and SAED pattern (g) of the Eu_2O_3 prepared from polymeric precursor PS-*co*-P4VP●$EuCl_3$ 1:5.

The TEM images of the pyrolytic EuOCl/Eu_2O_3 materials synthesized from the macromolecular precursor PS-*co*-P4VP●$EuCl_3$ in molar ratio 1:5 (see fig. 4e-f) showed bigger agglomerate sizes in which the bar-shaped nanomorphology can be also observed (see red squared regions in fig. 4e-f). Again, the SAED pattern (fig. 4g) suggested the

presence of nanocrystals of $EuOCl/Eu_2O_3$. The non-homogeneous sizes and shapes of the as-prepared $EuOCl/Eu_2O_3$ materials, is inconvenience consequence of the solid-state method to prepare these materials. Moreover, most of solid-state routes to nanostructured lanthanide oxides led to nanomaterials having bigger size and morphology dispersion than those created by solution methodologies[13].

2.3 SEM and TEM/HRTEM analysis of the as-prepared NdOCl materials.

SEM images of the as prepared NdOCl materials showed different grain structures. Thus, whereas grains of NdOCl obtained by pyrolysis of the macromolecular precursor Chitosan●$NdCl_3$ showed a cotton like texture (see SEM images of the 1:1 molar ratio precursor in fig. 5 a-c), grains of NdOCl from PS-*co*-P4VP●$NdCl_3$ exhibited very dense and compact textures (see for SEM images of the 1:1 precursor in fig. 5e-f). In both cases (Chitosan and PS-*co*-P4VP) the EDS analysis showed, as it is spected, the presence of Nd, Cl and O atoms (fig. 5d and 5g respectively).

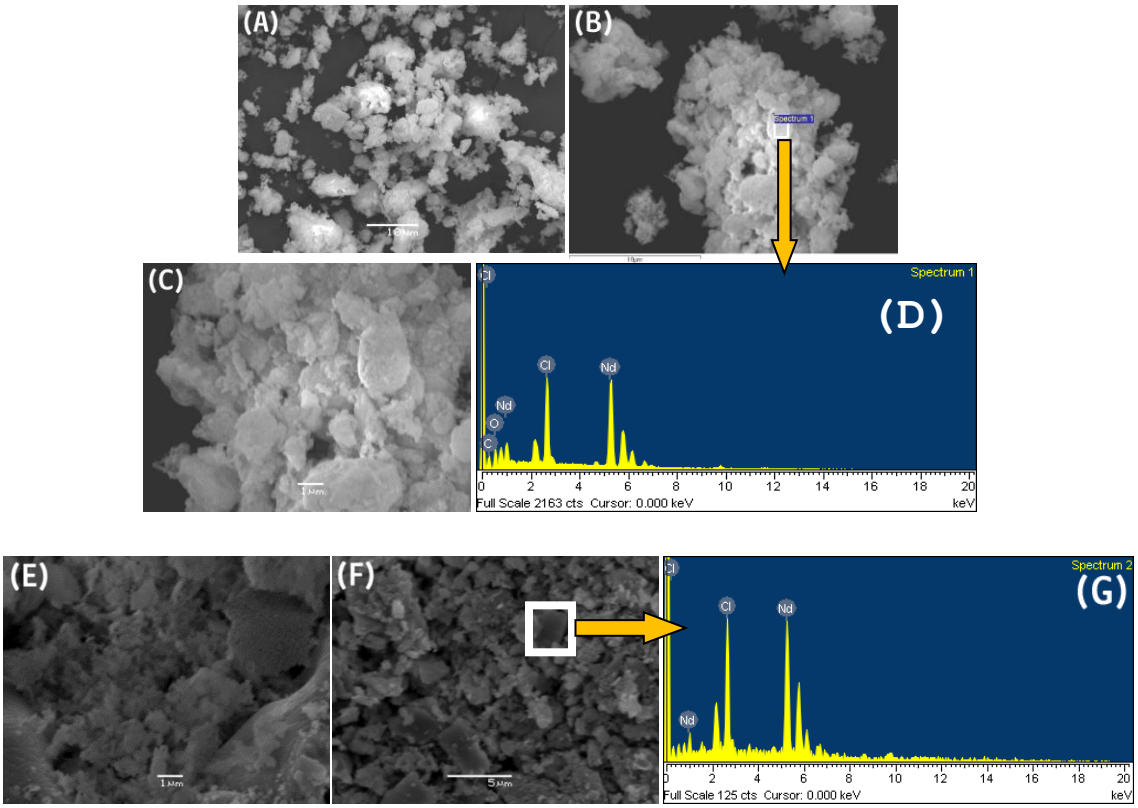

Fig. 5 (a)-(c) SEM images and EDS analysis (d) of the NdOCl materials prepared from the pyrolysis of the macromolecular precursors Chitosan●$NdCl_3$ 1:1. (e)-(f) SEM images and EDS analysis (g) of the NdOCl materials prepared by pyrolysis of the macromolecular precursor PS-*co*-P4VP●$NdCl_3$ in molar ratio 1:5.

Similarly to that previously observed in TEM images of the as-prepared Eu-containing materials, TEM pictures of NdOCl materials created by pyrolysis of Chitosan●$NdCl_3$ and PS-4-co-PVP●$EuCl_3$ (in both 1:1 and 1:5 molar ratios), exhibited the presence of NdOCl nanoparticles having not well defined morphologies and sizes (see TEM images of NdOCl prepared by pyrolysis of PS-*co*-P4VP●$NdCl_3$ in 1:5 or 1:1 molar ratios, in fig. 6a-c and fig. 6e-g respectively). Among the variety of different morphologies, concatenated structures, also observed with other solid-state thermal routes to these materials, were frequently observed (see fig. 6). SAED analysis of the as prepared NdOCl materials demonstrated the crystalline nature of these particles (see fig. 6d and 6h for SAED patterns of NdOCl from PS-*co*-P4VP●$NdCl_3$ 1:5 and 1:1 respectively).

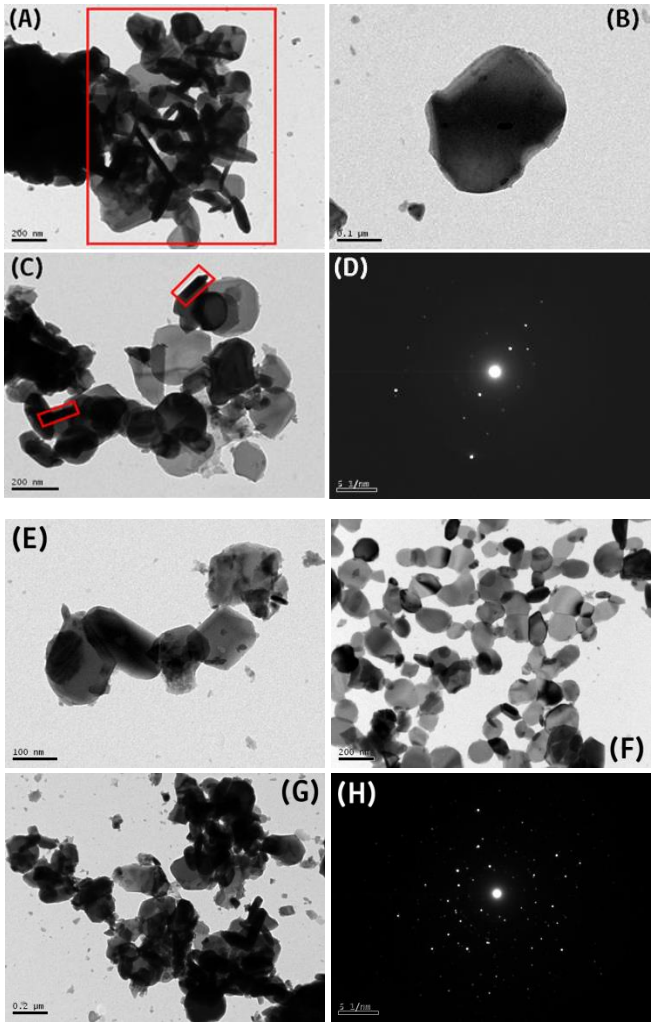

Fig. 6 TEM images [(a)-(c)] and SAED pattern (d) of NdOCl from PS-*co*-P4VP●$NdCl_3$ in 1:5 molar ratio. TEM images [(e)-(g)] and SAED pattern (h) of NdOCl from PS-*co*-P4VP●$NdCl_3$ in 1:1 molar ratio.

HRTEM images of NdOCl materials obtained from the pyrolysis of the macromolecular precursor Chitosan●$NdCl_3$ (1:1) are shown in Figure 7, in which *d*-spacing corresponding to the (001) and (101) planes of the NdOCl were clearly observed 0.678 nm and 0.346 nm (see fig. 7b and 7c). The SAED pattern (fig. 7d) showed the highly crystalline nature of the as prepared NdOCl materials. Importantly, the observed HRTEM features of the as-prepared NdOCl materials are in good agreement with those previously reported for nanostructured NdOCl materials prepared by solution methods [10,11].

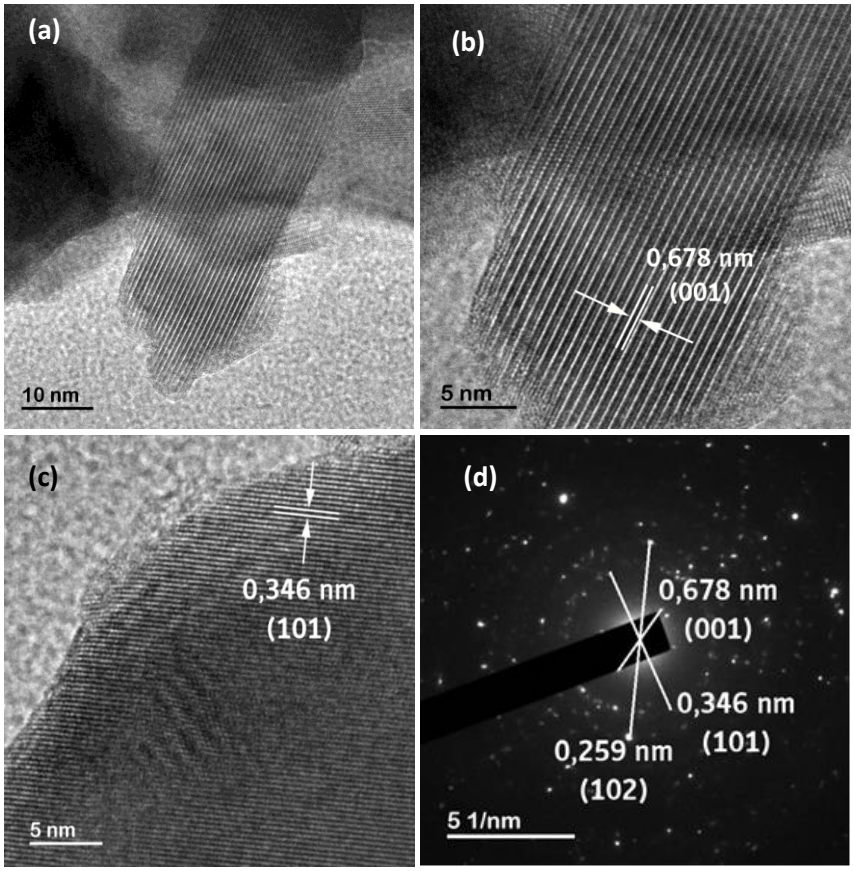

Fig. 7 HRTEM images (a)-(c) and selected-area electron diffraction (SAED) pattern (d) of the NdOCl materials obtained from the pyrolysis of Chitosan●$NdCl_3$ 1:1.

2.4 Photoluminescence studies of the $EuOCl/Eu_2O_3$

The emission photoluminescence analysis of the nanostructured $EuOCl/Eu_2O_3$ materials in the visible region, is shown in fig. 8.

Characteristic $^5D_0 \rightarrow {}^7F_n$ (n = 1, 2, 3, 4) transitions[24-28] were clearly observed for all as-prepared $EuOCl/Eu_2O_3$ materials. The intensity of the emission peaks is influenced by the nature of the polymeric support (Chitosan or PS-*co*-P4VP) as well as by the $LnCl_3$/polymer ratio (Ln = Eu, Nd. See fig. 8). Indeed, an enhanced intensity of emission peaks is observed when PS-*co*-P4VP was used as polymeric template, and 1:1 Nd/polymer

molar ratio was employed. This effect is explained by the higher porosity of the $EuOCl/Eu_2O_3$ materials created from PS-co-P4VP precursors having 1:1 molar ratios. Although, the emission spectra obtained for the as-prepared materials is rather similar to those obtained by using other solid-state synthetic methodologies[24], the emission peak at ca. 700 nm is less intense that that of other $EuOCl/Eu_2O_3$ materials created by solution methods [25-27]. Importantly, any energy emission dependence with the nature of the polymer precursor, neither with the metal/polymer ratio, was observed for the most intense peak of the spectra (maximum of the $^5D_0 \rightarrow {}^7F_2$ peak of the $EuOCl/Eu_2O_3$ materials prepared by all the macromolecular precursors were observed at 611.5 nm; 611 nm; 611,5 nm; and 611,56 nm respectively. See fig. 8),

In accordance to the excitation spectra of the as prepared $EuOCl/Eu_2O_3$ materials (see Appendices A2) a proposed assignment of the emission and absorption transitions is shown in figure 8b.

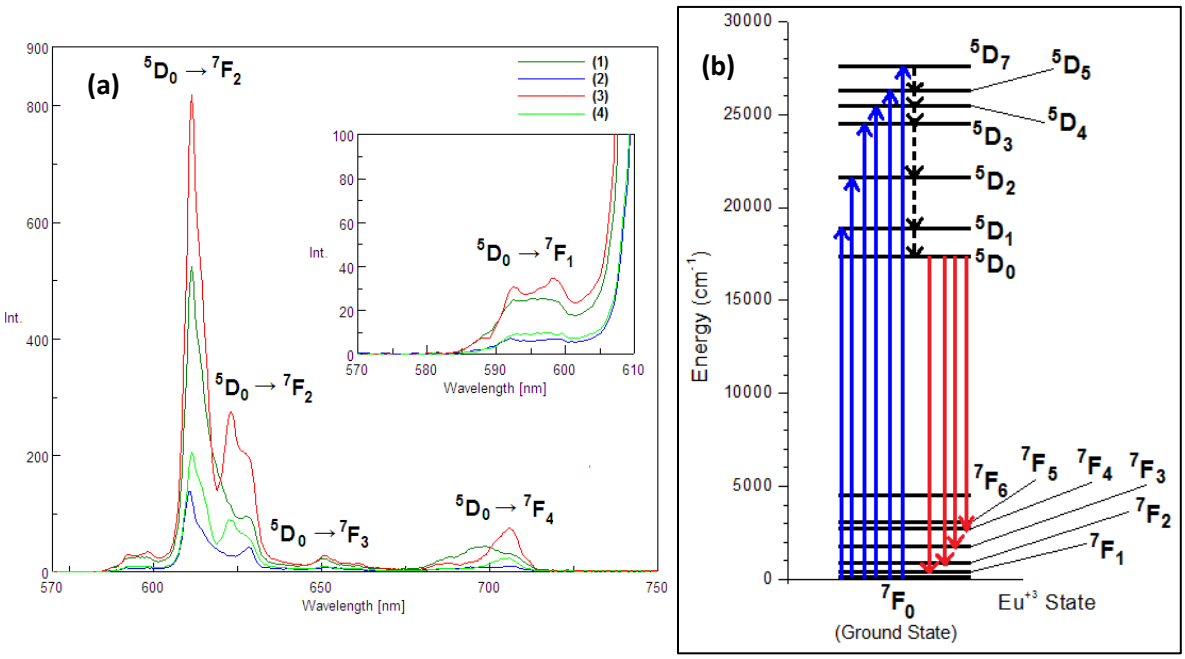

Fig. 8 Emission spectra of the products $EuOCl/Eu_2O_3$ obtained from precursors Chitosan●$EuCl_3$ and PS-*co*-P4VP●$EuCl_3$ in different metal /polymer molar ratios: (1) Chitosan●$EuCl_3$ (1:1); (2) Chitosan●$EuCl_3$ (1:5); (3) PS-*co*-P4VP●$EuCl_3$ (1:1); (4) PS-*co*-P4VP●$EuCl_3$ (1:5).

3 Conclusions

We described a solid-state route to NdOCl and $EuOCl/Eu_2O_3$ base on the pyrolysis of the very accessible macromolecular precursors Chitosan●$LnCl_3$ and PS-*co*-P4VP●$LnCl_3$

(Ln = Eu, Nd). Whereas the pyrolysis of the polymer●$NdCl_3$ (polymer = Chitosan and PS-*co*-P4VP) lead to nanostructure NdOCl with independence of the polymer/Nd molar ratio (1:1 or 1:5), mainly Eu_2O_3 pure phases were obtained by pyrolysis of Chitosan●$EuCl_3$ (1:1 and 1:5) and PS-*co*-P4VP●$EuCl_3$ (1:1). However, mixtures of EuOCl/Eu_2O_3 were obtained by pyrolysis of PS-*co*-P4VP●$EuCl_3$ (1:5). The texture of the lanthanide materials was influence by the nature of the polymeric template and the polymer/Ln molar ratio. For instance, whereas Eu_2O_3 materials having porous structure were obtained from PS-*co*-P4VP●$EuCl_3$ (1:1), foam textures were obtained from PS-*co*-P4VP●$EuCl_3$ (1:5). Moreover, NdOCl having cotton-like textures were obtained from Chitosan●$NdCl_3$ (1:1) whereas compacted grains were achieved by pyrolysis of PS-*co*-P4VP●$NdCl_3$ (1:1). The photoluminescence properties of the as prepared lanthanide a material was also influence by the nature of the polymeric support and the polymer/Ln molar ratio. Thus, an enhanced of the intensity of the emission peaks was observed when PS-*co*-P4VP was used as polymeric template, and when the 1:1 molar ratio was choosen. Then, Chitosan●$LnCl_3$ and PS-*co*-P4VP●$LnCl_3$ can be considered as accessible precursors to solid-state method leading to LnOCl materials. Therefore, the synthetic methodology described herein lead to Ln_2O_3 and LnOCl materials with similar features (sizes, morphology, emission properties, etc.) than those created by solution methods. However, our solid-state route do not need of tedious solvent evaporation steps, leading to desired lanthanide oxides with very good yields and in a straightforward manner. Moreover, this methodology the easy incorporation of lanthanide materials into solid-state electronic device as well in catalytic high temperature applied process.

Acknowledgements: This present work was supported by Fondecyt Project 1160241. A.P.S. is grateful to FICYT (SV-PA-13-ECOEMP-83, FC-15-GRUPIN14-106), Universidad de Oviedo (UNOV-13-EMERG-GIJON-08) and MINECO (CTQ2014-56345-P) for the funding. A.P.S. is also grateful to the COST (http://www.sips-cost.org/home/index.html), and the Juan de la Cierva and Ramón y Cajal programs.

References:

[1] Kort K R, Banerjee S. Shape-Controlled Synthesis of Well-Defined Matlockite LnOCl (Ln: La, Ce, Gd, Dy) Nanocrystals by a Novel Non-Hydrolytic Approach. *Inorg. Chem*., 2011, **50**: 5539.

[2] Du Y-P, Zhang Y-W, Sung L-D, Yan Ch-H. Atomically Efficient Synthesis of Self-assembled Monodisperse and Ultrathin Lanthanide Oxychloride Nanoplates. *J. Am. Chem. Soc.* 2009, **131**:3162.

[3] Walkers G, Parkin I P. The incorporation of noble metal nanoparticles into host matrix thin films: synthesis, characterisation and applications. *J. Mater. Chem.*, 2009, **19**:574.

[4] Pileni M P, Self-assembly of inorganic nanocrystals: fabrication and collective intrinsic properties. *Acc.Chem. Res.*, 2007, **40**:685.

[5] Pileni M P, 2D superlattices and 3D supracrystals of metal nanocrystals: a new scientific adventure. *J. Mater. Chem.*, 2011, **21**:16748.

[6] Wan Y F, Goubet N, Albouy P A, Pileni M P. Hierarchy in Au Nanocrystal Ordering in Supracrystals: A Potential Approach to Detect New Physical Properties. *Langmuir*, 2013, **29**:7456.

[7] Lee S-S, Park H-I, Joh Ch-H, Byon S-H. Morphology-dependent photoluminescence property of red-emitting *Ln*OCl:Eu (*Ln*=La and Gd). *J. Solid State Chemistry*, 2007, **180**:3529.

[8] Li G, Li Ch, Zhang C, Cheng Z, Quang Z. Peng Ch. Tm^{3+} and/or Dy^{3+} doped LaOCl monocrystalline phosphor for field emission displays. *J. Mater. Chem* , 2009,**19**:8936

[9] Mahajan S V, Hart J,.Everheart A, Redigholo M L,.Koktysh D S, Payzant E A. Synthesis of $RE(OH)_2Cl$ and REOCl (RE=Eu, Tb) nanostructures. *J.Rare Earths*, 2008, **26**:131.

[10] Li X, Deng X, Zhu H, Feng J, Peng Y, Bai J, Zheng X, Fan H, Wang M, Chen H. Well-Defined Flowerlike NdOCl Nanostructures: Nonaqueous Sol–Gel Synthesis, Nanoscale Characterization and Their Magnetic and Photoluminescence Properties. *Chem. An-Asian J*., 2014, **9**:584.

[11] Yue W, Xu X, Su Z, Irvine J T S, Zhou Y, Liu Y, Zhou W. Syntheses and proton conductivity of mesoporous Nd_2O_3–SiO_2 and NdOCl–SiO_2 composites. *J. Mater. Sci*. 2012, **47**: 2146.

[12] Wang M, Deng X, Feng J,Yu B, Zhu H, Li X, Zheng X, Bai J, Peng Y. Nonhydrolytic colloidal synthesis of ligand-capped single-crystalline NdOCl nanocubes and their magnetic properties. *J. Alloys and Comp.*, 2015,**619**:681.

[13] Díaz C, Valenzuela M L in "Metallic Nanostructures Using Oligo and Polyphosphazenes as Template or Stabilizer in Solid State" in Encyclopedia of Nanoscience and Nanotechnology, H.S Nalwa Ed., American Scientific Publishers; 2010, **16**, 239-256.

[14] Lee J, Zhang Q, Saito F. Mechanochemical Synthesis of LaO*X* (*X*=Cl, Br) and Their Solid State Solutions. *J. Sol. State Chemistry*, 2001, **160**:469.

[15] Yan Zheng-Guang, Yan Chun-Hua. Controled Synthesis of rare earth nanostructures *J. Mater. Chem*, 2008, **18**:5046.

[16] Tissue B M. Synthesis and Luminescence of Lanthanide Ions in Nanoscale Insulating Hosts. *Chem.Mater*., 1998, **10**:2837.

[17] Si R, Zhang Y W, Zhou H P, Sun L D, Yan Ch. Controlled-Synthesis, Self-Assembly Behavior, and Surface-Dependent Optical Properties of High-Quality Rare-Earth Oxide Nanocrystals. *Chem.Mater*., 2007, **19**:18.

[18] Shen Z, Zhan G, Zhou H, Sun P, Li B, Ding D, Chen T. Macroporous Lanthanide-Organic Coordination Polymer Foams and Their Corresponding Lanthanide Oxides. *Adv. Mater*., 2008, **20**:984.

[19] Díaz C, Barrera G, Segovia M, Valenzuela M L, Osiak M, O'Dwyer C. Crystallizing Vanadium Pentoxide Nanostructures in the Solid-State Using Modified Block Copolymer and Chitosan Complexes. *J. Nanomaterials*, 2015, **16**, Article No. 117, 13 pages.

[20] Díaz C, Barrientos L, Carrillo D, Valdebenito J, Valenzuela M L, Allende P, Geaney H, O'Dwyer C. Solvent-less method for efficient photocatalytic a-Fe_2O_3 nanoparticles using macromolecular polymeric precursors. *New J. Chem.*, 2016, **40**:6768.

[21] Díaz C, Platoni S, Molina A, Valenzuela M L, Geaney H, O'Dwyer C. Novel Solid-State Route to Nanostructured Tin, Zinc and Cerium Oxides as Potential Materials for Sensors. *Journal of Nanoscience and Nanotechnology*, 2014, **14**:6748.

[22] Díaz C, Valenzuela M L, Baez R, Segovia M. J Solid State Morphology and Size Tuninag of Nanostructured Platinum using Macromolecular Complexes. *J. Chil. Chem.Soc*., 2015, **60**:2986.

[23] Díaz C, Valenzuela M L, Rios C, Segovia M. Oxidation Facility by Temperature Dependence on the Metal Noble Nanostructured M°/M_xO_y Phase Products Using a Solid – Sate Method : The case of Pd . *J. Chil. Chem.Soc*., 2016, **61**:3014.

[24] Díaz C, Valenzuela M L, García C, De la Campa R, Presa A. Solid-state synthesis of pure and doped lanthanide oxide nanomaterials by using polymer templates. Study of their luminescent properties. *Materials Letters*, 2017, **209**:111.

[25] Bazzi R, Flores M A, Louis C, Lebbou K, Zhang W, Dujardin C, Roux S, Mercier B, Ledoux G, Bernstein E, Erriat P, Tillement O. Synthesis and properties of europium-based phosphors on the nanometer scale: Eu_2O_3, Gd_2O_3:Eu, and Y_2O_3:Eu. *J. Colloid Interface Sci*., 2004, **273**:191.

[26] Wakefield G, Keron H A, Dobson P J, Hutchison J L. Synthesis and Properties of Sub-50-nm Europium Oxide Nanoparticles. *J. Colloid Interface Sci*., 1999, **215**:179.

[27] Bazzi R, Flores M A, Louis C, Lebbou K, Dujardin C, Brenier A, Zhang W, Tillement O, Bernstein E, Perriat P. Synthesis and luminescent properties of sub-5-nm lanthanide oxides nanoparticles. *J. Luminescence*, 2003, **102-103**:445.

[28] P.K. Sharma, M.H. Jilavi, R. Mass, H. Schmidt, Tailoring the particles size from μm→nm scale by using a surface modifier and their size effect on the fluorescence properties of europium doped yttria. *J. Lumin.* 1999, **82:**187